U.S. GEOLOGICAL SURVEY

DEPARTMENT OF THE INTERIOR

Summary of natural remanent magnetization, magnetic susceptibility, and density measurements from the Lake City caldera area, San Juan Mountains, Colorado

by

V. J. S. Grauch and Mark R. Hudson

Denver, Colorado 80225

Open-File Report 87-182

1987

Table of Contents

	Page
INTRODUCTION	1
GEOLOGIC SETTING	3
MEASUREMENT TECHNIQUES	3
NRM	5
Magnetic Susceptibility	5
Density	5
DESCRIPTION OF TABLES	5
Magnetic-Property Tables	6
Density Tables	6
DISCUSSION	7
Magnetic-Property Data	7
Density Data	8
ACKNOWLEDGMENTS	9
REFERENCES CITED	9
APPENDIX: BRIEF DESCRIPTION OF GEOLOGIC UNITS	19

Page

LIST OF FIGURES

Figure 1. Location of Lake City area and sites 1SG-1 and 2SR-6 2

2. Location map of the calderas of the San Juan volcanic field 4

LIST OF TABLES

Table 1. List of site names and corresponding geologic units... 11

2. Summary of NRM data..... 13

3. Summary of susceptibility data..... 14

4. Total magnetization calculated from average NRM and induced magnetization vectors..... 15

5a. Summary of core density data..... 16

5b. Density data for single-sample sites..... 17

6. Average densities for geologic units..... 18

LIST OF PLATE

(in pocket)

Plate 1. Location of sampling sites

INTRODUCTION

This report summarizes natural remanent magnetization (NRM), magnetic susceptibility, and density measurements obtained from samples from the Lake City caldera area, San Juan Mountains, Colorado (Figure 1). These samples were collected as part of geochemical, geologic, magnetic, and gravity studies during the years 1981-1983. Other measurements of the magnetic properties of rocks in this area appear in Sheriff (1975), Lipman (1976), and Reynolds and others (1986). Extensive density measurements for this area have not been reported before. The intent of this summary is to present the data in a useful form for aeromagnetic and gravity interpretation.

Measurements from surface rocks may not reflect the integration of surface and subsurface properties that are measured by potential-field surveys. Lateral and vertical changes in rock composition, degree of alteration, and structural attitude are common in volcanic areas, suggesting that the magnetic properties and densities of rocks in such areas may also vary considerably. Nevertheless, the magnetic-property and density measurements from rocks of the Lake City caldera area, when used in conjunction with aeromagnetic and gravity information, are very useful in constraining the general properties of the rock units.

The distribution and representativeness of the rock magnetic and density data are primarily functions of the sampling goals of the collector, outcrop availability, suitability of the outcrop for sampling, and the number of sites sampled. Samples used in this study were collected for different purposes. Grauch (1SG sites) collected to get representative magnetic-property and density values for the area; Reynolds (1SR, 2SR, and 3SR sites) sampled as part of a paleomagnetic study of the history of resurgence (Reynolds and others, 1986); and D. Bove (Red Mountain core) and K. Hon (all other samples) collected for geochemical studies to further petrologic and geologic interpretations. Samples collected by Reynolds and Hon tend to be biased toward less rocks that exhibit little of the widespread alteration of the area. They may also include unique samples that best record the phenomena they were studying but are minor constituents of the geologic unit sampled.

Several factors determined the suitability of an outcrop: 1) the originality of the present position of the outcrop, 2) protection from lightning strikes, 3) coherence of the material to be sampled, and 4) sufficient jointing (if taking hand samples) so that the sample could be removed. Due to the ruggedness of the terrain in the Lake City area, sampling locations were restricted by accessibility as well as outcrop pattern. *In situ* outcrops are not abundant; most of the area is covered by rubble and vegetation. Outcrops occur as hills or cliffs of erosion-resistant, somewhat dense rocks, or are located in stream valleys. Outcrops are more abundant along the crests of high ridges, but these were avoided because of the likelihood that remanent magnetization would be affected by lightning strikes.

In general, sampling surface outcrops skew the results toward fresh rocks, which are denser and may be more magnetic (a lesser amount of magnetic minerals has been destroyed) than a truly representative suite of samples. However, surface exposures are subject to weathering, which may lower densities and reduce NRM and magnetic susceptibility values.

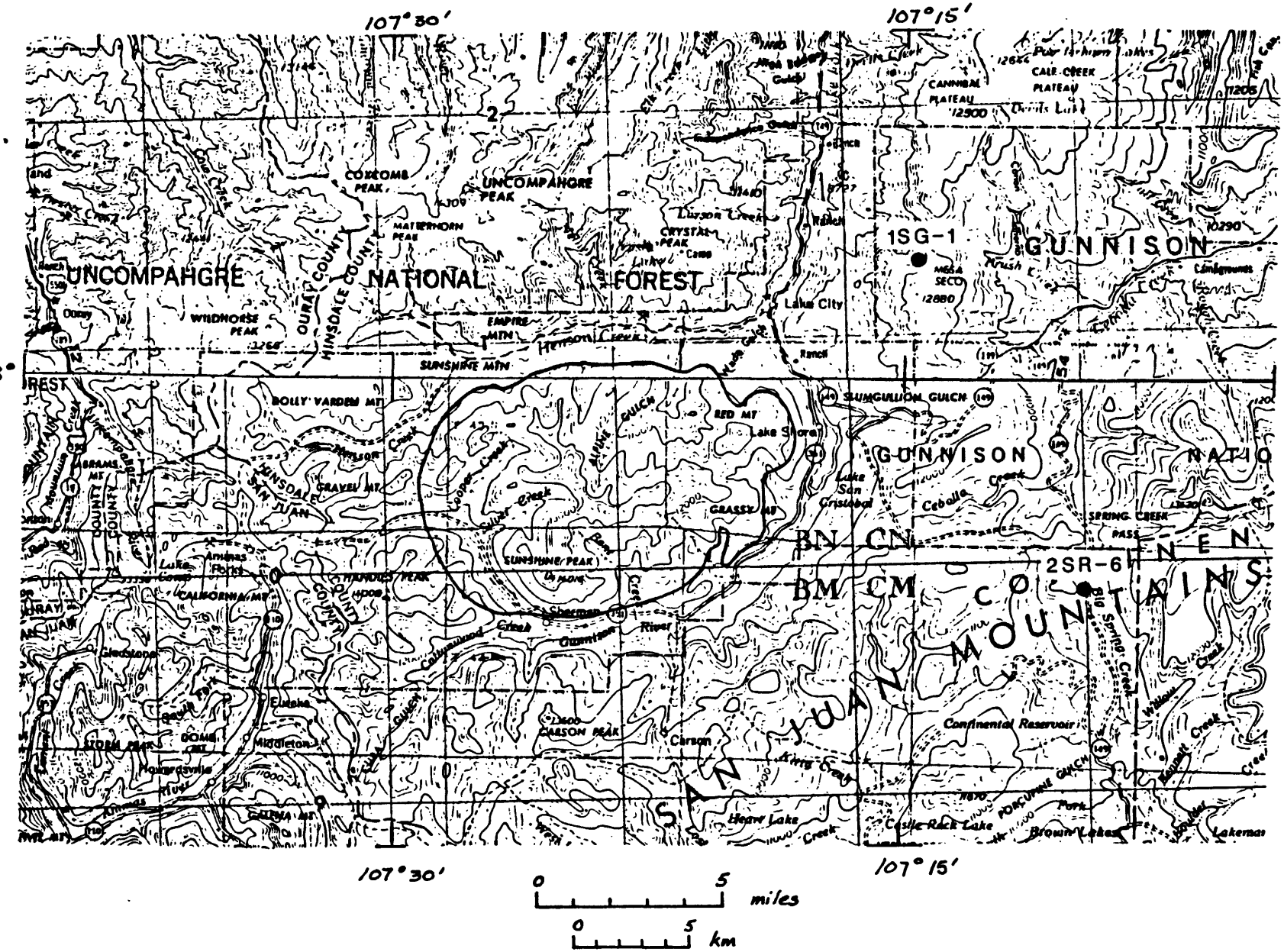

FIG. 1 -- Location of Lake City area and sites 1SG-1 and 2SR-1. Outline of Lake City caldera is shown schematically with heavy line.

GEOLOGIC SETTING

The Lake City caldera area is part of the San Juan volcanic field (Figure 2). The volcanic history of the San Juan Mountains spans approximately 35 m.y., from late Eocene to Holocene, and occurred in three main stages: (1) the extrusion of voluminous calc-alkalic andesites, (2) widespread caldera formation associated with the eruption of ash-flow tuffs, and (3) the eruption of primarily basaltic lavas (Steven and Lipman, 1976). All three phases of volcanic activity are represented in the Lake City caldera area.

Located in the western San Juan volcanic field, the Lake City caldera neighbors the Silverton caldera, which is to the southwest, and both are nested in an older caldera system that includes the Uncompahgre and San Juan calderas (Figure 2). During the rapid caldera formation of the second stage of San Juan volcanic activity, the Uncompahgre and San Juan calderas collapsed contemporaneously 28 m.a. and the Silverton caldera formed 27.5 m.a. (Steven and Lipman, 1976).

Eruption of the Sunshine Peak Tuff 23 m.a. resulted in the collapse of the Lake City caldera. This tuff characteristically contains abundant quartz phenocrysts and has a high silica content (Lipman and others, 1973). Hon (in press) has recognized three new members of the Sunshine Peak Tuff which are progressively more mafic from bottom to top: a lower (early) high-silica alkali rhyolite with 76% SiO_2, a middle rhyolite with 74% SiO_2, and an upper (late) quartz trachyte with 68% SiO_2. The major portion of the Sunshine Peak Tuff that is preserved occurs inside the Lake City caldera along with intracaldera breccias and sparse intracaldera lavas.

Resurgence of the Lake City caldera is evidenced by offsets between the Sunshine Peak Tuff members, doming of the tuff, and many outcrops of intrusive quartz syenite associated with resurgence Hon (in press). Measurements of remanent magnetization show that the ashflow tuffs, which predate but are compositionally associated with the quartz syenite, cooled rapidly during a period of reverse polarity of the Earth's magnetic field, preserving the reversed direction in their NRM. The quartz syenite intrusion cooled slowly as the Earth's field returned to normal polarity, acquiring a reverse-polarity remanence at high temperatures and a normal-polarity remanence at low temperatures (Reynolds and others, 1986). The normal-polarity component dominates the NRM.

Large amounts of dacite lava associated with the resurgent doming were extruded from ring fractures on the east side of the caldera and cooled during a reverse polarity of the Earth's field (Reynolds and others, 1986). These lava domes, composed of the dacite lavas of Grassy Mountain, totally obscure the ring fault on this side of the caldera. Extensive circulation of hydrothermal solutions propyllitized and silicified the units inside the caldera, primarily altering the rocks on the eastern side. The Red Mountain alunite deposit, located in one of the post-collapse lava domes, is purported to be the largest in the U.S. (Bove, 1984).

MEASUREMENT TECHNIQUES

Oriented samples were collected from <u>in situ</u> outcrops (sites). Hand samples were oriented using a bubble level and a magnetic or sun compass

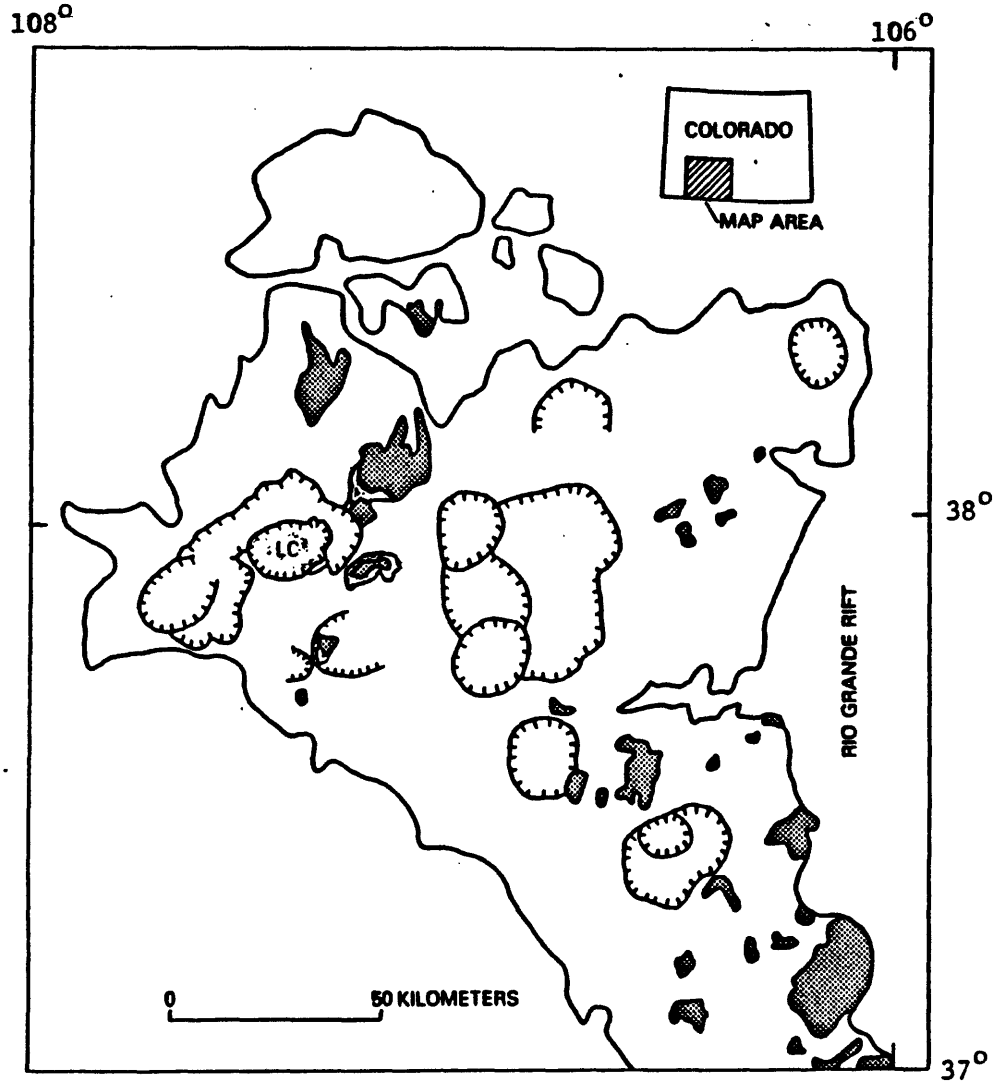

FIG. 2 -- Location map of the calderas of the San Juan volcanic field in southwestern Colorado. Calderas shown by hachured lines, LC=Lake City caldera; S = Silverton caldera. Outflow facies of the Sunshine Peak Tuff shown in light shading; Miocene basalts and basaltic andesites are darkly shaded. From Reynolds and others (1986).

before they were removed from the outcrop then later cored in the laboratory. Other samples were drilled by means of a portable rock drill at the site. In addition, some unoriented samples were collected. One or two cylindrical specimens, of radius 1 inch and approximately 1 inch in length, were cut from each core. NRM was measured from oriented specimens; susceptibil#ities were determined by dividing the weight of the dry sample by an estimate of its volume. The volume of each core was estimated by measuring it.

NRM

The direction and intensity of the NRM of core samples were measured using a 5 Hz spinner magnetometer whose sensitivity is 1×10^{-7} emu/cm^3. All specimens were allowed to spin until a signal-noise ratio of 40:1 was achieved. The directions of NRM were reproducible to 1-2°, and the maximum error in repeatability of the magnetization is less than 2%. Intensities were converted to units of emu/cm^3 by dividing by the volume of the specimen, which was estimated by measuring the core radius and height.

Magnetic Susceptibility

Volume susceptibilities were obtained from core samples by means of a highly sensitive bridge system whose noise level is 2×10^{-8} in the cgs system (Christie and Symons, 1969). Maximum errors in repeatability for the Lake City data were on the order of 1%.

Density

Dry bulk densities were determined by dividing the weight of the dry sample by an estimate of its volume. The volume of each core was estimated by measuring its radius and height. The volume of irregular hand samples was determined by a water-displacement technique: The weight of water, containing vessel, and rock suspended in the water minus the weight of water and vessel without the rock, divided by the density of water (1.00 g/cm^3), equals the volume of water displaced, or the volume of the rock. Maximum errors from both these techniques are estimated to be ±0.02 g/cm^3.

DESCRIPTION OF TABLES

Table 1 lists the sites where cored samples were collected; uncored samples are listed with the density measurements on Table 5b. The locations of all sites are plotted on Figure 1 or Plate 1. For cored samples, the first number of the site name is the last digit of the year the site was sampled; for instance, 2 refers to 1982. The next two letters refer to the sampling area (S = San Juan Mountains) and the field party leader (G=Grauch, R=Reynolds). The last number indicates the order in which the sites were sampled that year. Reynolds and others (1986) used different site names for some of the same sites; these names are also listed on Table 1 where applicable. In addition, Table 1 lists the unit codes and geologic unit names; detailed descriptions are in the Appendix. Descriptions and classifications of the geologic units are from Hon (in press) and Lipman (1976).

Magnetic-Property Tables

The NRM measurements of samples from each site were averaged and summarized on Table 2. If more than one specimen was measured from a single hand sample, then the average of the specimen values was counted as one sample value. The mean remanent direction and associated semi-angle of the cones of 95% confidence (α_{95}) were determined by the method Fisher (1953). For a constant number of samples, the larger α_{95} becomes, the greater the scatter in the vector directions. The range, average and standard deviation of the intensities for the samples are also shown on Table 2.

Some samples were not used because their directions were wildly inconsistent with other samples from the same site. These samples may have been (1) misoriented, (2) sampled from a slumped or rotated block, (3) struck by lightning, giving rise to an isothermal remanent magnetization (IRM), or (4) affected to varying degrees by acquisition of secondary chemical or viscous remanent magnetizations (CRM or VRM).

The volume susceptibility measurements of all the samples at each site were averaged and are summarized on Table 3. If more than one specimen was measured from a single hand sample, then the average of the specimen values was counted as one sample value. In addition to the average, Table 3 shows the range and standard deviation at each site.

Table 4 summarizes the magnetic-property data for each geologic unit. The data are separated as induced, NRM, and total magnetization vectors. For the induced component, the average susceptibility (in the cgs system) is an average of all the site averages. The induced intensity* (in units of emu/cm^3) is the average susceptibility multiplied by the Earth's field of 0.541 Oersteds (54,100 gammas) for the Lake City area. The direction of the induced vector parallels the Earth's field for the area (declination 12.5^o and inclination 65^o) in 1979, the time when a detailed aeromagnetic survey was flown over the area (High Life Helicopters/QEB, 1981).

The average remanent direction was computed for each site by using the site averages of Table 3 in Fisher's (1953) method. The average NRM intensity was computed linearly from site averages. The Koenigsberger ratio (Q) is the ratio of NRM to induced intensity; it shows the relative contributions of the remanent and induced components to the total magnetization. The total magnetization vector is calculated by vectorially adding the average NRM vector to the average induced vector.

Density Tables

Table 5a summarizes the density measurements of all the cored samples at each site. If more than one specimen was measured from a single hand sample, the average of the specimen values was counted as one sample value. The range and standard deviations are also shown. Table 5b lists the density values of the uncored samples (only one or two were collected for each site).

*In this report, the terms intensity and magnetization are used interchangeably and both denote the magnitude of the magnetization vector. The intensity in emu/cm^3 is converted to System International (SI) units of A/m by multiplying by 10^3 (Shive, 1986).

Table 6 summarizes the density data for each geologic unit, and lists which samples were averaged to represent that unit. Very low density values in the middle and upper members of the Sunshine Peak Tuff (Tspm and Tspu) may indicate welding breaks (K. Hon, written commun., 1986). Therefore, two very low density values were excluded from the averages and result in significantly higher density averages (Table 6).

The single-sample density values for the quartz syenite (Tisy) are considered to be most representative of the fresh rock. The other samples are biased toward more altered rock and/or are close to the edges of the intrusion where some of the ashflow tuff was assimilated into the intrusion (K. Hon, oral commun., 1987). These processes tend to lower original density values.

DISCUSSION

Magnetic-Property Data

NRM directions from Table 2 that are generally consistent for one geologic unit also have relatively low values for α_{95}. Conversely, a large scatter in directions (high α_{95}) generally corresponds to low remanent intensities, as is the case for the unit Tisy. This scatter renders a poor estimate of representative NRM vectors on Table 4, but these small-magnitude vectors have insignificant contributions to the estimate of the total magnetization vectors.

A common supposition in aeromagnetic work is that all total magnetizations in an area are effectively collinear with the Earth's present field direction. The supposition permits the use of aeromagnetic filtering operations based on this assumption, such as reduction-to-pole and pseudogravity transformation. The total magnetization vector $\vec{M}_T$ may be expressed in the cgs system as

$$\vec{M}_T = \vec{M}_R + k\vec{B}, \qquad (1)$$

where $\vec{M}_R$ is the NRM vector, k is susceptibility, and $\vec{B}$ is the Earth's field vector. Bath (1968) suggests that a difference of less than 25° from collinearity between $\vec{M}_R$ and $\vec{B}$, either in the same or opposite sense, qualifies the collinearity assumption, that is,

$$\vec{M}_T \simeq (M_R + kB)\,\hat{B}, \qquad (2)$$

where $\hat{B}$ is the unit vector in the direction of the Earth's field, and M_R is positive or negative depending on whether the collinearity is in the same or opposite sense, respectively. We suggest that a better rule of thumb compares the collinearity of the total magnetization vector and the Earth's field direction. Using the total magnetization vector instead of the NRM vector takes into account the significance of the NRM magnitude in the vector addition. For instance, on Table 4 units Tiqm and Tisy have NRM directions significantly different from the induced direction, whereas their NRM intensities are so small that the total magnetization vectors are closely approximated by equation (2). The units Tidrp and Tspu have NRM directions that are within 25° of being collinear in the opposite sense with the induced vector (Table 4), but their total magnetization vectors differ significantly from the induced directions and should <u>not</u> be approximated by equation (2).

Most of the units listed on Table 4 have total magnetization vectors that can be approximated by equation (2). Magnetizations for the units Tidrp, Tldg, Tspu, and Tspm must be treated vectorially by equation (1).

Rock units can be further classified into groups based on the intensity of their total magnetization (Bath and Jahren, 1984):

$<5x10^{-5}$ emu/cm^3	nonmagnetic
$5x10^{-5}$ - $5x10^{-4}$ emu/cm^3	weakly magnetic
$5x10^{-4}$ - $1.5x10^{-3}$ emu/cm^3	moderately magnetic
$>1.5x10^{-3}$ emu/cm^3	strongly magnetic

Inspection of Table 4 shows that Tiqm and Tmp are strongly magnetic; Tap is moderately magnetic; the rest are weakly magnetic. As expected, positive aeromagnetic anomalies are associated with the three moderately to strongly magnetic units (Grauch, in press).

Density Data

As mentioned previously, hydrothermal alteration is probably the largest factor in lowering the density values of the two averages for Tisy on Table 6. The lower averages for Tspu and Tspm (Table 6) may be skewed by inclusion of low-density samples from welding breaks within ash-flow sheets. Such rocks are not uncommon, but do not represent a significant volume of the rock (K. Hon, oral commun., 1986). The outflow portion of Tspl has a much lower density than the intra-caldera Tspl rocks; it should be treated as a separate unit.

The average densities shown on Table 6 can be used to estimate a reduction density* for the gravity survey of Grauch and Campbell (1985), which primarily covers geologic units within the Lake City caldera. The most prevalent geologic units that crop out within the caldera are Tspl, caldera collapse breccias, and various surficial deposits (Hon, in press). The surficial deposits are neither laterally nor vertically very extensive (Hon, in press), so can be considered negligible in their effect on most of the gravity measurements. The collapse breccias are dominantly composed of broken blocks of intermediate-composition volcanic rocks (Hon, in press). The bulk density of the breccias is probably somewhat less than that of an average dacite (2.58 g/cm^3; Telford and others, 1976); the estimate would be close to the density estimates for Tspl (2.50-2.53). The hornfels rocks of Tspl occur near contacts with the resurgent intrusion; the fresh Tspl rocks are considered to be more representative of the whole area. Thus, a good reduction density for the gravity survey is 2.50 g/cm^3.

*Use of dry bulk densities to estimate reduction density presumes that the gravitational effects of porosity and large cracks and holes in the in situ rocks are negligible. One can safely assume that porosity in the welded tuffs of the area is small. However, the voids or fluid-filled spaced provided by fracturing at depth may require a representative density that differs significantly from dry bulk density of the rock. This error cannot be adequately estimated from surface fracture patterns.

Another method for determining a reduction density is by the Nettleton profiling method (Telford and others, 1976), which uses a profile of gravity measurements over a topographic feature composed of one geologic unit. Different reduction densities are tested to give several gravity profiles. The density whose profile has the least correlation with the topographic feature (i.e., the topographic effects have been properly removed) is chosen as the proper reduction density.

The results of Nettleton profiling reported by Grauch and Campbell (1985) suffered from out-of-date geologic mapping; the stations chosen were not located on the same geologic unit. Unfortunately, it is still not possible to choose more than three closely spaced gravity stations located on the same geologic unit (as defined presently by Hon, in press). Therefore, the average density of 2.50 for fresh Tspl given here is considered a better estimation of the reduction density than 2.40, as given by Grauch and Campbell (1985).

ACKNOWLEDGMENTS

Many people helped collect these samples, including Dana Bove, Neil Fishman, Ken Hon, Denise Mruk, Rich Reynolds, and Charlie West. We are grateful to Dana Bove and Ken Hon for use of their density data. Ken Hon helped immensely with geologic information about the area.

REFERENCES CITED

Bath, G. D., 1968, Aeromagnetic anomalies related to remanent magnetism in volcanic rock, Nevada Test Site: Geological Society of America Memoir 110, p. 135-146.

Bath, G. D., and Jahren, C. E., 1984, Interpretation of magnetic anomalies at a potential repository site located in the Yucca Mountain area, Nevada Test Site: U.S. Geological Survey Open-File Report 84-120, 40 p.

Bove, D. J., 1984, Geology and hydrothermal alteration of the Red Mountain alunite deposit, Lake City, Colorado [abs.]: Geological Society of America Abstracts with Programs, v. 16, no. 4, p. 216.

Caskey, D. J., 1979, Geology and hydrothermal alteration of the Iron Beds area, Hinsdale County, Colorado: University of Texas at Austin, unpub. M. Sc. thesis, 111 p.

Christie, K. W., and Symons, D. T. A., 1969, Apparatus for measuring magnetic susceptibility and its anisotropy: Geological Survey of Canada Paper 69-41, 10 p.

Fisher, R. A., 1953, Dispersion on a sphere: Proceedings of the Royal Society of London, v. A217, p. 295-305.

Grauch, V. J. S., in press, Interpretive aeromagnetic map using the horizontal gradient: Lake City caldera area, San Juan Mountains, Colorado: U.S. Geological Survey Geophysical Investigations Map GP-974, scale 1:48,000.

Grauch, V. J. S., and Campbell, D. L., 1985, Gravity survey data and a Bouguer gravity anomaly map of the Lake City caldera area, Hinsdale County, Colorado: U.S. Geological Survey Open-File Report 85-208, 11 p.

High Life Helicopters/QEB, 1981, Contour maps of uranium, uranium/thorium ratio and total field magnetics, Lake City Area, San Juan Mountains, Colorado; with an introduction by Willian D. Heran: U.S. Geological Survey Open-File Report 81-568, 22 p.

Hon, Ken, in press, Geology, alteration, and mineralization of the Redcloud Peak (Lake City caldera) and Handies Peak wilderness study areas, Hinsdale County, Colorado: U.S. Geological Survey Miscellaneous Field Studies Map MF_ , scale 1:24,000.

Lipman, P. W., 1976, Geologic map of the Lake City caldera area, western San Juan Mountains, southwestern Colorado: U.S. Geological Survey Miscellaneous Investigations Map I-962, 1:48,000.

Lipman, P. W., Steven, T. A., Leudke, R. G., and Burbank, W. S., 1973, Revised volcanic history of the San Juan, Uncompahgre, Silverton, and Lake City calderas in the western San Juan Mountains, Colorado: U.S. Geological Survey Journal Research, v. 1, no. 6, p. 627-642.

Reynolds, R. L., Hudson, M. R., and Hon, Ken, 1986, Paleomagnetic evidence regarding the timing of collapse and resurgence of the Lake City caldera, San Juan Mountains, Colorado: Journal of Geophysical Research, v. 91, no. B9, p. 9599-9613.

Sheriff, S. D., 1975, Paleomagnetism of the San Juan volcanic field, southwestern Colorado: Master's Thesis, Western Washington State College, Bellingham, Washington, 113 p.

Shive, P. N., 1986, Suggestions for the use of SI units in magnetism: EOS, v. 67, no. 3, p. 25.

Slack, J. F., 1980, Multistage vein ores of the Lake City district, western San Juan Mountains, Colorado: Economic Geology, v. 75, no. 7, p. 963-991.

Steven, T. A., and Lipman, P. W., 1976, Calderas of the San Juan volcanic field, southwestern Colorado: U.S. Geological Survey Professional Paper 958, 35 p.

Telford, W. M., Geldart, L. P., Sherriff, R. E., and Keys, D. A., 1976, Applied Geophysics: Cambridge University Press: Cambridge.

TABLE 1. LIST OF SITE NAMES AND CORRESPONDING GEOLOGIC UNITS

SITE NAME	REYNOLDS & OTHERS	UNIT CODE	GEOLOGIC UNIT NAME
MIOCENE ROCKS OF THE LAKE CITY CALDERA			
1SG-5	QM-1	Tiqm	quartz monzonite of Alpine Gulch
3SR-6	QR-1	Tidrp	dacite porphyry of Red Mountain
1SR-1	SY-1		
1SR-6	SY-2	Tisy	quartz syenite (resurgent intrusion)
1SG-3	SY-3		
1SG-6	QG-4		
1SG-7	N/A		
1SG-8	QG-5	Tldg	dacite lavas of Grassy Mountain
2SR-8	QG-1		
3SR-5	QG-2		
3SR-7	QG-3		
1SG-17	SPU-6		
1SR-2	SPU-1		
2SR-1	SPU-2	Tspu	upper member of the Sunshine Peak Tuff
2SR-2	SPU-3		
3SR-2	SPU-4		
3SR-3	SPU-5		
1SG-13	N/A		
1SG-14	N/A		
1SR-3	SPM-1	Tspm	middle member of the Sunshine Peak Tuff
2SR-3	SPM-2		
3SR-1	SPM-3		
3SR-4	SPM-4		
1SG-2	SPL-1	Tspl	lower member of the Sunshine Peak Tuff
1SG-1	SPO-2	Tspl	lower member of the Sunshine Peak Tuff
2SR-6	SPO-1	(outflow)	

TABLE 1. LIST OF SITE NAMES AND CORRESPONDING GEOLOGIC UNITS (continued)

SITE NAME	REYNOLDS & OTHERS	UNIT CODE	GEOLOGIC UNIT NAME
OLIGOCENE ROCKS OF THE UNCOMPAHGRE CALDERA			
1SG-16	N/A	Tmp	25 to 28 m.y.-old monzonitic stock
1SR-5	N/A	Tap	porphyritic unit of the pyroxene andesite member of the Silverton Volcanics
1SG-10	N/A		
1SG-11	N/A		
1SG-12a	N/A	Tbb	Burns Member of the Silverton Volcanics
1SG-12b	N/A		
1SG-15	N/A	Tse	Eureka Member of the Sapinero Mesa Tuff

See Appendix for description of geologic units. Locations of sites plotted on Plate 1 and Figure 1.

TABLE 2. SUMMARY OF NRM DATA

UNIT CODE	SITE	NO. OF SAMPLES	AVE.[1] DEC	AVE.[1] INC.	α_{95}	RANGE INTENSITY[2] MIN.	MAX.	AVERAGE INTENSITY[2]	STD. DEV.[2] INTENSITY
Tiqm	1SG-5	8	75.9	37.1	101.7	1.51×10^{-5}	1.15×10^{-4}	6.51×10^{-5}	3.8×10^{-5}
Tidrp	3SR-6	7	242.4	-82.1	29.8	3.4×10^{-4}	1.50×10^{-3}	1.08×10^{-3}	0.47×10^{-3}
	1SR-1	9	165.2	10.7	38.1	7.47×10^{-7}	3.71×10^{-4}	5.47×10^{-5}	12.0×10^{-5}
Tisy	1SR-6	9	324.3	70.4	17.4	3.07×10^{-7}	2.96×10^{-5}	1.03×10^{-5}	1.2×10^{-5}
	1SG-3	7	47.0	-39.2	*	1.80×10^{-7}	9.06×10^{-6}	3.31×10^{-6}	3.22×10^{-6}
	1SG-6	7	175.8	-35.6	4.6	1.26×10^{-4}	2.41×10^{-4}	1.92×10^{-4}	0.38×10^{-4}
	1SG-7	6	180.3	-37.5	5.7	1.30×10^{-3}	2.89×10^{-3}	2.10×10^{-3}	0.66×10^{-3}
Tldg	1SG-8	5	162.0	-36.3	7.0	3.1×10^{-5}	1.53×10^{-4}	8.02×10^{-5}	5.1×10^{-5}
	2SR-8	7	152.5	-52.5	20.5	4.3×10^{-5}	5.83×10^{-4}	1.89×10^{-4}	1.9×10^{-4}
	3SR-7	7	110.5	-39.8	5.3	4.03×10^{-4}	2.00×10^{-3}	8.44×10^{-4}	5.69×10^{-4}
	1SG-17	7	154.1	-45.8	12.1	5.26×10^{-5}	1.40×10^{-3}	4.66×10^{-4}	5.94×10^{-4}
	1SR-2	7	145.0	-38.7	15.5	6.4×10^{-5}	2.45×10^{-4}	1.52×10^{-4}	0.59×10^{-4}
	2SR-1	6	27.3	-30.1	50.2	7.40×10^{-6}	3.70×10^{-5}	2.35×10^{-5}	1.24×10^{-5}
Tspu	2SR-2	8	329.4	-26.9	19.8	1.70×10^{-5}	4.18×10^{-5}	3.02×10^{-5}	0.89×10^{-5}
	3SR-2	6	175.4	-56.8	3.8	2.06×10^{-4}	9.54×10^{-4}	5.37×10^{-4}	3.6×10^{-4}
	3SR-3	7	169.8	-54.3	4.0	9.69×10^{-5}	3.26×10^{-3}	8.64×10^{-4}	12.0×10^{-4}
	1SG-13	5	76.0	-69.6	7.8	1.18×10^{-5}	6.05×10^{-5}	3.82×10^{-5}	2.0×10^{-5}
	1SG-14	6	42.6	-67.8	20.3	3.81×10^{-5}	5.30×10^{-5}	4.84×10^{-5}	0.55×10^{-5}
Tspm	1SR-3	9	115.7	-30.9	7.3	1.90×10^{-4}	3.45×10^{-4}	3.89×10^{-4}	3.21×10^{-4}
	2SR-3	6	141.7	-43.6	3.1	4.49×10^{-4}	9.04×10^{-4}	7.05×10^{-4}	2.09×10^{-4}
	3SR-1	7	103.2	-56.8	5.0	1.53×10^{-3}	5.19×10^{-3}	2.41×10^{-3}	1.30×10^{-3}
	3SR-4	7	163.8	-18.6	22.4	2.08×10^{-5}	7.52×10^{-5}	4.33×10^{-5}	1.97×10^{-5}
Tspl	1SG-2	6	101.0	-51.2	7.5	4.17×10^{-5}	8.71×10^{-5}	6.23×10^{-5}	1.61×10^{-5}
Tspl	1SG-1	7	116.1	-72.9	28.1	1.69×10^{-5}	9.36×10^{-5}	3.38×10^{-5}	2.7×10^{-5}
outflow	2SR-6	5	93.6	-61.0	4.6	8.00×10^{-6}	1.42×10^{-5}	9.02×10^{-6}	2.9×10^{-6}
Tmp	1SG-16	6	261.4	69.6	14.5	2.76×10^{-4}	3.57×10^{-4}	3.14×10^{-4}	0.36×10^{-4}
Tsp	1SR-5	8	186.2	-20.6	*	4.37×10^{-4}	1.17×10^{-3}	7.09×10^{-4}	2.56×10^{-4}
Tbb	1SG-11	3	188.6	-56.9	13.5	2.5×10^{-4}	1.52×10^{-3}	7.37×10^{-4}	6.85×10^{-4}
	1SG-12A	3	187.8	-51.5	8.2	9.7×10^{-4}	1.54×10^{-4}	1.32×10^{-4}	0.31×10^{-4}
Tse	1SG-15	3	148.3	-55.6	6.2	5.5×10^{-5}	1.43×10^{-4}	1.05×10^{-4}	0.45×10^{-4}

[1]Declination is measured in degrees east of N; inclination in degrees down from horizontal
[2]All intensities are in emu/cm^3. Multiply by 10^3 to convert to SI units (A/m)
*Unable to calculate α_{95} due to large scatter

TABLE 3. SUMMARY OF SUSCEPTIBILITY DATA

UNIT CODE	SITE	NO. OF SAMPLES	RANGE SUSCEPTIBILITY MIN.	MAX.	AVERAGE SUSCEPTIBILITY	STD. DEVIATIO SUSCEPTIBILIT
Tiqm	1SG-5	6	1.799×10^{-3}	4.085×10^{-3}	3.11×10^{-3}	0.94×10^{-3}
Tidrp	3SR-6	8	1.304×10^{-3}	1.657×10^{-3}	1.49×10^{-3}	0.12×10^{-3}
	1SR-1	15	6.933×10^{-5}	1.861×10^{-3}	1.12×10^{-3}	0.56×10^{-3}
Tisy	1SR-6	7	5.103×10^{-4}	2.284×10^{-3}	1.38×10^{-3}	0.64×10^{-3}
	1SG-3	8	1.531×10^{-5}	8.803×10^{-5}	3.28×10^{-5}	2.75×10^{-5}
	1SG-6	8	1.046×10^{-4}	2.327×10^{-4}	1.51×10^{-4}	0.50×10^{-4}
	1SG-7	6	6.253×10^{-5}	2.688×10^{-4}	1.47×10^{-4}	0.75×10^{-4}
	1SG-8	5	2.877×10^{-4}	5.922×10^{-4}	3.89×10^{-4}	1.32×10^{-4}
Tldg	2SR-8	7	1.243×10^{-4}	7.607×10^{-4}	3.82×10^{-4}	2.44×10^{-4}
	3SR-5	5	1.694×10^{-3}	7.764×10^{-3}	3.43×10^{-3}	2.50×10^{-3}
	3SR-7	7	3.342×10^{-4}	7.942×10^{-4}	5.85×10^{-4}	1.41×10^{-4}
	1SG-17	7	1.408×10^{-3}	1.999×10^{-3}	1.54×10^{-3}	0.20×10^{-3}
	1SR-2	11	1.101×10^{-3}	1.643×10^{-3}	1.33×10^{-3}	0.19×10^{-3}
Tspu	2SR-1	5	6.063×10^{-5}	8.487×10^{-4}	6.37×10^{-4}	3.33×10^{-4}
	2SR-2	7	1.426×10^{-3}	1.711×10^{-3}	1.58×10^{-3}	0.11×10^{-3}
	3SR-2	5	6.688×10^{-4}	8.297×10^{-4}	7.65×10^{-4}	0.67×10^{-4}
	3SR-3	7	7.733×10^{-5}	7.103×10^{-4}	3.46×10^{-4}	2.67×10^{-4}
	1SG-13	6	3.475×10^{-5}	6.122×10^{-5}	5.66×10^{-5}	1.75×10^{-5}
	1SG-14	6	8.261×10^{-5}	2.506×10^{-4}	1.40×10^{-4}	0.71×10^{-4}
	1SR-3	9	1.474×10^{-4}	7.935×10^{-4}	3.24×10^{-4}	2.00×10^{-4}
Tspm	2SR-3	5	5.474×10^{-4}	7.119×10^{-4}	6.17×10^{-4}	0.78×10^{-4}
	3SR-1	8	7.563×10^{-4}	9.846×10^{-4}	8.37×10^{-4}	0.84×10^{-4}
	3SR-4	7	2.709×10^{-4}	4.764×10^{-4}	3.69×10^{-4}	0.75×10^{-4}
Tspl	1SG-2	7	6.102×10^{-5}	9.502×10^{-5}	7.69×10^{-5}	1.18×10^{-5}
Tspl	1SG-1	9	2.821×10^{-4}	7.891×10^{-4}	5.40×10^{-4}	1.39×10^{-4}
outflow	2SR-6	6	6.547×10^{-5}	7.126×10^{-5}	6.88×10^{-5}	0.24×10^{-5}
Tmp	1SG-16	6	2.723×10^{-3}	4.029×10^{-3}	3.30×10^{-3}	0.49×10^{-3}
Tap	1SR-5	8	2.945×10^{-3}	3.669×10^{-3}	3.37×10^{-3}	0.25×10^{-3}
	1SG-10	3	2.181×10^{-3}	2.524×10^{-3}	2.32×10^{-3}	0.18×10^{-3}
	1SG-11	3	5.888×10^{-5}	6.542×10^{-4}	2.69×10^{-4}	3.34×10^{-4}
Tbb	1SG-12a	3	1.834×10^{-5}	1.064×10^{-4}	7.33×10^{-5}	4.79×10^{-5}
	1SG-12b	2	2.496×10^{-3}	3.616×10^{-3}	3.06×10^{-3}	0.79×10^{-3}
Tse	1SG15	5	2.297×10^{-4}	6.120×10^{-4}	4.74×10^{-4}	1.52×10^{-4}

All susceptibilities are in the cgs system. Multiply by 4π to convert to SI

Table 4. Total magnetization calculated from average NRM and induced magnetization vectors.

	INDUCED COMPONENT			NRM COMPONENT[2]				TOTAL MAGNETIZATION					
UNIT CODE	No. Sites	Ave. Suscept. (cgs units)	Intensity[1] (emu/cm^3)	No. Sites	Ave. Dec.	Ave. Inc.	Ave. Inten. (emu/cm^3)	Q	Dec.	Inc.	Intensity (emu/cm^3)	Diff.[3] Rem/In	Diff.[3] Tot/In
Tiqm	1	3.11×10^{-3}	1.68×10^{-3}	1	(75.9	37.1	6.51×10^{-5})	0.04	16.1	64.8	1.73×10^{-3}	45.8	1.5
Tidrp	1	1.49×10^{-3}	8.06×10^{-4}	1	242.4	-82.1	1.08×10^{-3}	1.33	347.6	-51.5	4.34×10^{-4}	159.2	118.0
Tisy	3	8.44×10^{-4}	4.57×10^{-4}	3	(103.5	37.8	2.28×10^{-5})	0.05	17.8	65.7	4.70×10^{-4}	56.7	2.3
Tidg	6	8.47×10^{-4}	4.58×10^{-4}	5	157.7	-43.1	6.81×10^{-4}	1.49	139.6	-8.0	3.59×10^{-4}	150.8	112.2
Tspu	6	1.03×10^{-3}	5.59×10^{-4}	6	135.7	-73.3	3.56×10^{-4}	0.64	37.9	39.7	2.59×10^{-4}	159.2	29.3
Tspm	6	3.91×10^{-4}	2.11×10^{-4}	6	121.7	-54.0	6.06×10^{-4}	2.87	107.2	-41.5	4.51×10^{-4}	144.6	128.8
Tspl	3	2.29×10^{-4}	1.24×10^{-4}	3	101.6	-61.9	3.50×10^{-5}	0.28	29.9	55.9	9.8×10^{-5}	142.8	12.5
Tmp	1	3.30×10^{-3}	1.79×10^{-3}	1	261.4	69.6	3.14×10^{-4}	0.18	4.4	69.3	2.04×10^{-3}	37.2	5.3
Tap	1	3.37×10^{-3}	1.82×10^{-3}	1	(186.2	-20.6	7.08×10^{-4})	0.39	45.7	84.6	1.41×10^{-3}	135.4	20.7
Tbb	4	1.43×10^{-3}	7.74×10^{-4}	2	188.2	-54.2	4.35×10^{-4}	0.56	27.0	77.7	3.57×10^{-4}	169.0	13.4
Tse	1	4.74×10^{-4}	2.56×10^{-4}	1	148.3	-55.6	1.05×10^{-4}	0.41	44.6	61.9	1.65×10^{-4}	156.8	14.5

[1]Susceptibility times the Earth's field vector having declination 12.5°, inclination 65.0°, intensity 0.541 Oe.

[2]Values in parentheses indicate poor estimates of a representative NRM vector due to influence of large scatter (see Table 2).

[3]Rem/In indicates difference between the direction of the remanent vector and the induced vector in degrees. Tot/In indicates difference between the direction of the total magnetization vector and the induced vector in degrees. Angles $\leq 25°$ and between 335° and 360° indicate the vectors are within 25° of being parallel; angles between 155° and 205° indicate they are within 25° of being collinear in the opposite sense.

TABLE 5a. SUMMARY OF CORE DENSITY DATA

UNIT CODE	SITE	NO. OF SAMPLES	RANGE DENSITY MIN.	MAX.	AVERAGE DENSITY	STD. DEV. DENSITY
Tiqm	1SG-5	6	2.52	2.57	2.54	0.02
Tidrp	3SR-6	9	2.45	2.57	2.51	0.04
	1SR-1	9	2.27	2.40	2.34	0.04
Tisy	1SR-6	7	2.37	2.54	2.45	0.06
	1SG-3	8	2.44	2.51	2.48	0.02
	1SG-6	8	2.38	2.49	2.44	0.04
	1SG-7	6	2.21	2.38	2.31	0.06
	1SG-8	6	2.42	2.50	2.45	0.03
Tldg	2SR-8	8	2.41	2.58	2.51	0.06
	3SR-5	5	2.45	2.57	2.50	0.04
	3SR-7	7	2.29	2.54	2.43	0.11
	1SG-17	7	2.22	2.50	2.37	0.09
	1SR-2	7	2.27	2.42	2.37	0.05
	2SR-1	9	1.85	1.99	1.93	0.01
Tspu	2SR-2	6	2.18	2.20	2.19	0.01
	3SR-2	6	2.34	2.44	2.39	0.04
	3SR-3	7	2.34	2.46	2.41	0.05
	1SG-13	4	2.33	2.41	2.37	0.04
	1SG-14	4	2.37	2.44	2.42	0.03
Tspm	1SR-3	9	2.33	2.44	2.38	0.03
	2SR-3	5	2.15	2.27	2.20	0.05
	3SR-1	8	1.87	2.19	2.01	0.11
	3SR-4	7	2.21	2.63	2.40	0.14
Tspl	1SG-2	6	2.47	2.53	2.50	0.02
Tspl	1SG-1	9	1.86	1.93	1.89	0.03
outflow	2SR-6	6	1.84	1.91	1.86	0.07
Tmp	1SG-16	6	2.47	2.53	2.50	0.02
Tap	1SR-5	8	2.41	2.53	2.50	0.04
	1SG-10	3	2.27	2.34	2.30	0.04
	1SG-11	3	2.20	2.26	2.23	0.03
Tbb	1SG-12a	3	2.22	2.31	2.28	0.05
	1SG-12b	2	2.45	2.49	2.47	0.03
Tse	1SG-15	5	2.25	2.36	2.29	0.04

All densities are in g/cm^3

TABLE 5B. DENSITY DATA FOR SINGLE-SAMPLE SITES

Tspl
LOWER MEMBER OF
SUNSHINE PEAK TUFF

SITE	DENSITY
Fresh Samples	
2-6-14	2.57
5-2C-126	2.47
5-2C-127	2.49
6-1-35	2.49*
RC-2-108	2.59
RC-2-158	2.59
RC-3-1	2.59
RC-3-61	2.25
RC-3-68	2.47
RC-4-45	2.48
Hornfels Samples	
12250 CT	2.56
2-6-28	2.56
RC-2-20	2.31
RC-2-24	2.56
RC-2-41	2.54
RC-2-48	2.59
RC-2-73	2.57
RC-2-103	2.53
RC-2-104	2.56
RC-2-160	2.55

Tisy
QUARTZ SYENITE
RESURGENT INTRUSION

SITE	DENSITY
2-6-13	2.61
RC-2-5	2.60
RC-2-159	2.62

Tldg
DACITE LAVAS OF
GRASSY MOUNTAIN

SITE	DENSITY
Average**	2.53

All densities are in g/cm^3.

*Average of two samples.

**Data only available as an average of 3 samples (D. Bove, written comm., 1987)

TABLE 6. Average Densities for Geologic Units

UNIT	WHICH SITES	NO. SITES	AVERAGE DENSITY
Tiqm	All	1	2.54
Tidrp	All	1	2.51
Tisy	All	6	2.52
Tisy	single-sample	3	2.61
Tldg	All	7	2.45
Tspu	All	6	2.28
Tspu	excl. 2SR-1*	5	2.35
Tspm	All	6	2.30
Tspm	excl. 3SR-1*	5	2.35
Tspl	Fresh + Hornfels	21	2.52
Tspl	Fresh	11	2.50
Tspl	Hornfels	10	2.53
Tspl	outflow	2	1.88
Tmp	All	1	2.50
Tap	All	1	2.50
Tbb	All	4	2.32
Tse	All	1	2.29
Red Mt.**	All	21	2.35

All density values are in g/cm^3.

*All samples used exclusive of the one listed.

**Suite of samples collected at the surface and from core drilled on Red Mt. by D. Bove (written comm., 1987) that represents an average section through the variably altered geologic units of the mountain.

APPENDIX. BRIEF DESCRIPTION OF GEOLOGIC UNITS

The following geologic descriptions of the map units listed on Table 1a are condensed from Hon (in press) and Lipman (1976).

MIOCENE ROCKS OF THE 23.1-M.Y.-OLD LAKE CITY CALDERA

Tiqm — QUARTZ MONZONITE OF ALPINE GULCH--Porphyritic quartz monzonite (67 to 68% SiO_2) intruded near the mouth of Alpine Gulch. Composed of large (.25 to .75 inch), euhedral prismatic phenocrysts of pink microperthitic orthoclase set in a subhedral holocrystalline matrix of sodic plagioclase, orthoclase, quartz, biotite, and clinopyroxene. Alteration of the quartz monzonite is weak and consists of partial sericitization of plagioclases, partial chloritization of biotites, and nearly total replacement of clinopyroxene by chlorite.

The quartz monzonite is believed to have been intruded late in the caldera cycle, comagmatic with the dacite of Red Mountain (K. Hon and Z. C. Peng, unpub. data). Remanent magnetic polarity: normal. K-Ar age 22.8 $\pm$ 0.9 m.y.

DACITE OF RED MOUNTAIN--Complex of porphyritic, high-K dacite intrusions that cut the postcollapse lavas in the vicinity of Red Mountain. Probably the near-surface feeders for a volcanic dome complex.

Tidrp — Dacite Porphyry--Porphyritic dikes of high-K dacite (63 to 65% SiO_2) to the northeast and south of Red Mountain. The dikes contain about 40 to 45 percent phenocrysts of plagioclase, sanidine, biotite, clinopyroxene, and opaques in a crypto- to microcrystalline groundmass composed largely of plagioclase feldspar and quartz. Alteration is weak in the dikes, which show only minor sericitization of plagioclase and partial conversion of clinopyroxene to chlorite and calcite. Mineralogically, petrologically, and isotopically similar to the quartz monzonite of Alpine Gulch. Remanent magnetic polarity: reverse

RESURGENT INTRUSIONS--Stocks, dike-like bodies, small plugs, and ring-fracture dikes of quartz syenite and related rhyolitic rocks. Represent the uppermost parts of a large resurgent intrusion that underlies the northcentral part of the Lake City caldera. Mineralogically and chemically similar to equivalent compositions of the Sunshine Peak Tuff.

Tisy — Quartz syenite--Seriate-porphyritic, quartz syenite (64 to 69% SiO_2). Phenocrysts include microperthitic orthoclase (generally 20 to 30%), plagioclase (5 to 20%), biotite, clinopyroxene, and opaques. Large (.3 to .5 inch), glomeroporphyritic plagioclase is

scattered throughout the quartz syenite. Accessory phases include sphene, zircon, apatite, and chevkinite.

The groundmass of the phaneritic intrusions in the caldera is typically a hypidiomorphic granular intergrowth of quartz and potassium feldspar. Quartz syenite dikes intruded along the ring fault generally have higher silica contents (67 to 69% SiO_2) than the holocrystalline quartz syenites within the caldera (64 to 66% SiO_2).

Quartz-bearing granite porphyry (72 to 74% SiO_2) locally forms the borders of flat-topped, phaneritic quartz syenite intrusions in the center of the caldera. This border phase only occurs along contacts where the quartz syenite appears to have partially assimilated hornsfelsed lower Sunshine Peak Tuff.

Alteration with the quartz syenite commonly consists of weak to moderate sericitization of plagioclase, partial chloritization of biotite, and replacement of clinopyroxene by either uralitic hornblende or by chlorite, calcite, and epidote. K-Ar age 23.3 $\pm$ 1 m.y. Remanent magnetic polarity: normal below 500 degrees Celsius; reverse at higher demagnetization temperatures (Reynolds and others, 1986).

Tldg DACITE LAVAS OF GRASSY MOUNTAIN--Seriate-porphyritic, high-K dacite lavas (63 to 66% SiO_2) occurring as thick flows and probable domal masses on the eastern margin of the caldera. Contain 40 to 45% phenocrysts of plagioclase (20 to 25%), sanidine (5 to 10%), biotite, clinopyroxene, and opaques. Zircon and apatite are accessory phases. Groundmass is generally a cryptocrystalline granular intergrowth of quartz and feldspar, but locally patchy granophyric crystallization has occurred. The dacite lavas are characterized by high modal concentrations of mafic minerals (averages 12%) in comparison to other caldera related rocks.

Alteration is generally weak away from Red Mountain and consists of oxidation of biotite, minor sericitization of plagioclase, weak argillization of groundmass, and replacement of clinopyroxene by smectite with or without chlorite and calcite. In the vicinity of Red Mountain, the lavas are totally replaced by an assemblage of quartz and alunite that grades outward into a moderately argillized zone (Bove, 1984). Thickness exceeds 2000 feet in places. K-Ar age 23.4 $\pm$ 1.2 m.y. Remanent magnetic polarity: reverse.

SUNSHINE PEAK TUFF--Compositionally zoned intracaldera ash-flow sheet consisting of three ash-flow members that interfinger complexly with a caldera-collapse breccia member. The ash-flow members contain variable amounts of xenolithic rocks fragments, which have lithologies similar to those in the collapse breccia member. Individual ash-flow tuff members have mineralogical and chemical equivalents in the resurgent intrusions.

Tspu Upper member--Quartz trachytic ash-flow tuff (67 to 69% SiO_2). Crystal-rich, moderately to densely welded ash-flow tuff containing 45 to 50% phenocrysts of sanidine, plagioclase, biotite, quartz, clinopyroxene, and opaques in a matrix of devitrified glass shards. Locally, the upper member has a thin (<50 feet), quartz-rich basal zone that is rhyolitic (72% SiO_2). Accessory phases include sphene, zircon, apatite, and rare chevkinite (where preserved from alteration). Distinguished from other members by relatively low quartz phenocryst content (<5%) and more abundant plagioclase (5 to 10%) and biotite (1 to 3%).

Prominent welding breaks are present within the upper member in the southern part of the caldera. Degree of welding within the upper member adjacent to breaks is highly variable. The tuff can be densely welded to its base, where a thin quenched zone (<20 feet) of microspherulitic devitrification is developed. Poorly to moderately welded tuff also occurs adjacent to or in places defining breaks, especially where the basal layer is lithic rich.

Alteration within the upper member is generally weak in comparison to the other two members. Mild sericitic alteration has affected much of the plagioclase, and all of the clinopyroxene is pseudomorphed by calcite, chlorite, and clay. In the vicinity of Red Mountain, the upper member has been completely replaced by quartz and alunite.

Total thickness of the upper member is at least 1500 feet. Thins to less than 500 feet to the north of Grassy Mountain, apparently due to erosion prior to the eruption of the postcollapse dacite lavas. K-Ar age 23.2 $\pm$ 1.2 m.y. Remanent magnetic polarity: reverse

Tspm Middle member--Rhyolitic ash-flow tuff (73 to 75% SiO_2). Contains 35 to 45% phenocrysts of sanidine, quartz, plagioclase, biotite, clinopyroxene, and opaques in a moderately to densely welded matrix of glass shards. Accessory minerals include sphene, zircon, apatite, and chevkinite. Distinguished from the lower member by the presence of plagioclase and large (up to .05 inch) biotite flakes (about 1%), and from the upper member by higher quartz content (5 to 12%).

Prominent welding breaks separate the middle member into two cooling units near the head of Alpine Gulch and into three cooling units in the northwestern part of the caldera. These breaks are marked by lithic-rich (20 to 50%), poorly welded ash-flow tuff. The middle and lower members are separated by a sheet of caldera-collapse breccia through most of the southern half of the caldera. Where the middle member rests on this breccia unit, it commonly is zoned from nonwelded tuff (10 to 15 feet thick) into densely welded tuff that is locally vitrophyric.

Propylitic alteration has affected large areas of the middle member, but exposures in the southeastern aprt of the caldera are relatively fresh. Thickness of the middle member is approximately 1000 feet. K-Ar age 24.0 $\pm$ 0.9 m.y. Remanent magnetic polarity: reverse

Tspl Lower member--High-silica rhyolitic ash-flow tuff (76% to 77% SiO_2). Contains 30 to 40% phenocrysts of microperthitic orthoclase and elliptical quartz with minor biotite, clinopyroxene, and opaques set in a groundmass of thoroughly devitrified glass shards. Sphene, zircon, apatite, and chevkinite occur in trace amounts. Adjacent to and above many of the quartz syenite intrusions, the lower member has been recrystallized to a dense hornfels.

Most of the intracaldera lower member has been propylitized, and only samples of the hornfelsed tuff have major-element chemistry similar to unaltered samples of outflow lower member. Strong hydrothermal alteration occurs over large areas of the lower member, especially in association with quartz veining.

The lower member is more than 2500 feet thick in the center of the caldera and no base has been identified. K-Ar age is 22.4 $\pm$ 1.2 m.y. Remanent magnetic polarity: reverse

OLIGOCENE ROCKS OF THE UNCOMPAHGRE CALDERA

MONZONITE PORPHYRY--Moderately to coarsely porphyritic intrusive rocks having phaneritic fine-grained groundmass. Phenocrysts are mostly plagioclase accompanied by augite and biotite. These rocks are characterized by plagioclase, clinopyroxene, orthopyroxene, and variable amounts of biotite. K-Ar ages are between 25 and 28 m.y. (Slack, 1980; Caskey, 1979). Remanent magnetic polarity: Normal

SILVERTON VOLCANICS--Lava flows of intermediate to silicic composition and related volcaniclastic sedimentary rocks that accumulated within the Uncompahgre caldera after its collapse, but before subsidence of the Silverton caldera

Pyroxene andesite member--Andesitic lava flows that largely overlie the Burns Member but locally interfinger complexly with it.

Tap — Porphyritic andesite--Coarsely porphyritic andesite containing 15-25 percent phenocrysts of plagioclase and augite. Thin tabular flows averaging 10-20 m thick that occur exclusively in northern parts of the Uncompahgre and San Juan calderas and attain a maximum thickness of about 250 m.

Burns Member--Relatively silicic lava flows ranging from hornblende rhyodacite to biotite rhyolite.

Tbb — Biotite-quartz latite--Thick flows and domes containing 15-30 percent phenocrysts of plagioclase, biotite, and augite. Locally at least 300 m thick.

SAPINERO MESA TUFF--Rhyolitic ash-flow sheet, erupted from the San Juan and Uncompahgre calderas about 29 m.y. ago, and related caldera-collapse breccia

Tse — Eureka Member (intracaldera)--Moderately-welded to densely-welded tuff containing 5 to 20 percent phenocrysts of plagioclase, sanidine, and biotite, propylitized in lower part. Typically contains numerous small angular fragments of andesite and sparse blocks of older welded tuffs